nature geoscience
SUPPLEMENTARY INFORMATION
DOI: 10.1038/NGEO1987

Contribution of ocean overturning circulation to tropical rainfall peak in the Northern Hemisphere

Observations of Surface Heat Fluxes and Oceanic Energy Transports

Ocean heat storage with global warming and natural variability complicates the relation between surface fluxes and ocean heat transport (OHT). The vertically integrated ocean energy budget is

$$dO/dt + \mathrm{div}\, F = -S$$

where O is the ocean heat content, F is the OHT, and S is the upward surface heat flux from ocean to atmosphere. We obtain the cross-equatorial OHT estimate by integrating the equation from pole to equator, assuming that dO/dt term is equal in the NH and SH. Could differences in ocean heat uptake between hemispheres cause a significant modification to our cross-equatorial OHT estimate? Estimates of ocean heat content changes have been calculated in as done in ref.S1, and we examine the heat uptake within the upper 700 m of the ocean over the time period 2001-2010. Estimating the dO/dt term over the top 700 m of ocean with a linear trend over the time period of record gives a global mean heat uptake of 0.13 PW. The NH-SH difference in heat uptake is much smaller, -0.007 PW, and thus does not significantly affect our estimate of cross-equatorial transport of 0.4 PW assuming uniform heat uptake. Data from the top 2000 m of ocean is only available since 2005, but the NH-SH difference from 2005-2011 is -0.0005 PW,

DOI: 10.1038/NGEO1987

so again makes a negligible contribution to our estimate. The observed heat content change of the ocean has been remarkably symmetric between hemispheres over recent decades.

Meridionally integrating the basin zonal mean net surface flux (which in the time mean equals the basin meridional OHT divergence) provides the meridional OHT for each basin (Fig. S1). The northward cross-equatorial OHT occurs in the Atlantic, a well-known result established both indirectly and directly[S2-S4]. The cross-equatorial OHT in the Pacific is near zero, while in the Indian Ocean there is a southward cross-equatorial OHT that is smaller than the northward transport in the Atlantic. Hence the global mean is northward.

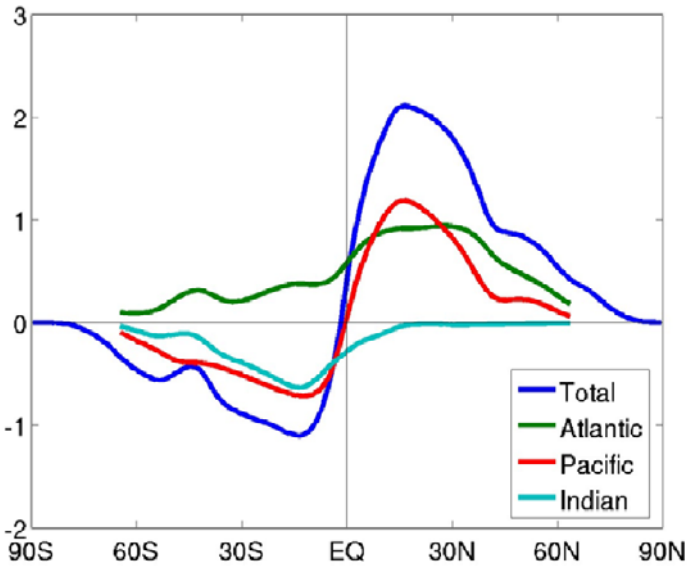

Figure S1. Northward OHT in different basins (in PW). Calculated based on the method of ref.S9.

Poleward Atmospheric Energy Transports

To facilitate comparison of magnitudes, we plot the atmospheric poleward moist static energy transport in the NH and SH on the same curve in Fig. S2.

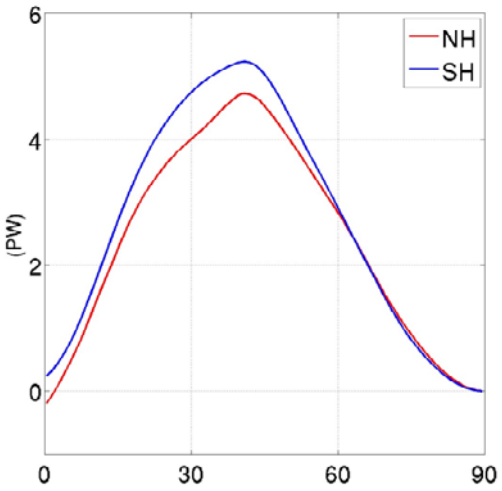

Figure S2. Poleward transport of moist static energy in the SH (blue) and NH (green). From ERA-Interim data, calculated based on the method of ref.S10.

Idealized Model Simulations

The simulations presented in the red line in Fig. 1c and this section are performed with an aquaplanet (ocean-covered) version of GFDL AM2.1[S5], modified for zonal symmetry of forcings as in ref.S6. A similar aquaplanet configuration has been used with idealized surface heat flux prescriptions[S6, S7]; in this study we add the seasonal cycle of solar radiation, and use a slab ocean

DOI: 10.1038/NGEO1987

heat capacity of 2.5×10^8 J/m^2/K, corresponding to 60 m depth of water. The simulation in Fig. 1c uses this model with the observed surface heat flux from Fig. 2d as a lower boundary forcing (often called a "Q-flux").

Additional experiments with the aquaplanet model show that the extratropical surface heat flux is most important for the tropical precipitation pattern. A nearly identical peak precipitation location occurs when observed asymmetric heat fluxes only outside of 20^o are specified, while using hemispherically symmetrized, zonally averaged tropical fluxes (Fig. S3, red solid line). The zonal mean precipitation responses are not sensitive to the longitudinal structure of the prescribed Q-flux in the extratropics (as discussed in ref.S8). The results also vary little when prescribing the zonal mean extratropical Q-flux (Fig. S3, red dashed line).

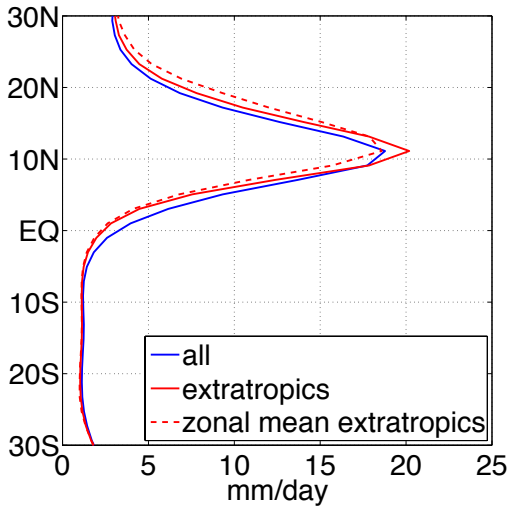

Figure S3. The zonal mean precipitation in aquaplanet AM2 experiments prescribing (a) the observed Q-flux (blue solid line), as in Fig.1c, (b) the observed Q-flux in the extratropics, with zonally averaged and hemispherically symmetrized Q-flux in the tropics (red solid line), and (c) the zonally averaged observed Q-flux in the extratropics with zonally averaged and hemispherically symmetrized Q-flux in the tropics (red dashed line).

GCM Simulations with Full Continental Geometry

The simulations presented in the grey lines in Fig. 1c and this section are performed with the ECHAM GCM version 4.6 with realistic geography. In Fig. 1c, we demonstrated that the observed OHT is essential for the northward displacement of the tropical rain band. In this section, we perform two simulations using the model's default Q-flux to show that removing the hemispheric asymmetry in the model's Q-flux also results in a southward displacement of the tropical rain band. The control case here uses the model's standard Q-flux, which includes a seasonal cycle. Note the zonal mean precipitation in the control run is closer to observations compared with the run with observed surface heat flux (compare Fig. 1b, 1c, and Fig. S4), as the model's standard Q-flux is derived from a fixed sea surface temperature simulation that matches the observed sea surface temperature. The symmetrized case uses a surface flux distribution that is zonally symmetric, with values chosen at each latitude such that the zonal integral of the surface flux is equal to the average between the NH and SH zonal integrals of the model's default Q-flux.

The latitude-longitude distribution of precipitation for all four cases with the ECHAM model are shown in Fig. S5. In both set-ups, the symmetrization of the surface flux weakens the NH ITCZ at all longitudes within the Pacific and Atlantic Basins, and strengthens the SH ITCZ within the eastern Pacific and Atlantic. The Indian Ocean basin responds rather differently, with a split into two ITCZ structures in both cases. This suggests a rather different dependence of Indian Ocean rainfall on the asymmetry of OHT, perhaps with the tropical OHT playing a larger

DOI: 10.1038/NGEO1987

role. Such sensitivities should be analyzed with more regional surface flux modification experiments, and in coupled GCMs.

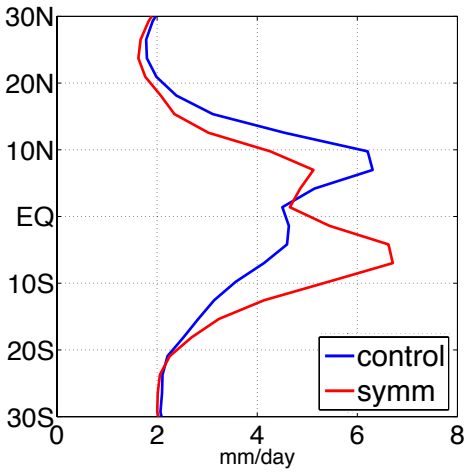

Figure S4. The zonal mean precipitation in ECHAM experiment prescribing (a) the default Q-flux in the model (blue solid line) and (b) the hemispherically symmetrized Q-flux (red solid line).

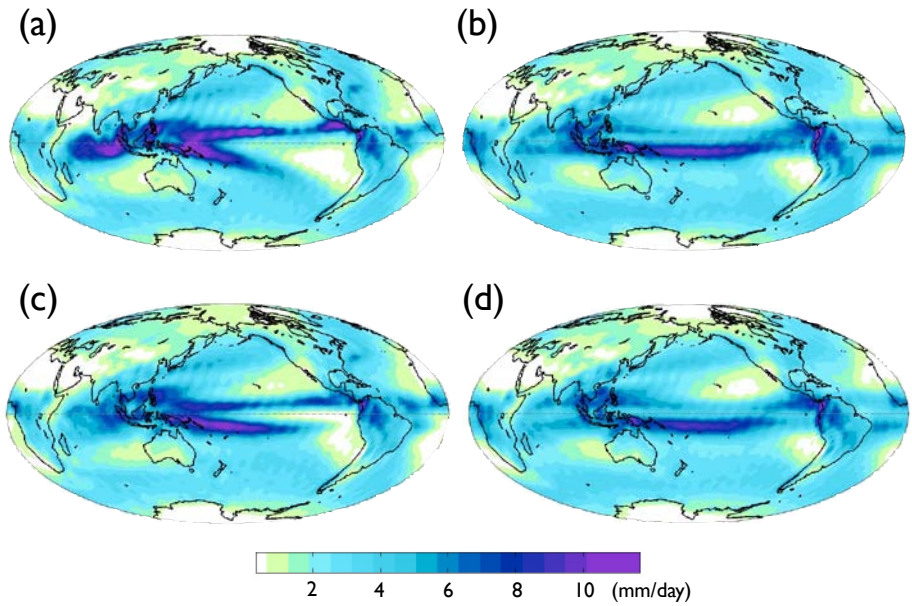

Figure S5. Time mean precipitation distribution in simulations with the ECHAM model prescribing different surface flux distributions. (a) Default model Q-flux distribution, (b) hemispherically symmetrized default Q-flux distribution, (c) observed surface flux distribution, (d) hemispherically symmetrized observed surface flux distribution.

Hemispheric Asymmetry in Surface Heat Fluxes in GCMs

CMIP5	NH minus SH upward Surface flux (W/m^2)	CMIP3	NH minus SH upward Surface flux (W/m^2)
BCCcsm1	3.2	MIROC hires	1.9
CanESM2	1.6	MRI CGCM2	4.2
CCSM4	4.1	MIROC medres	3.5
CNRMcm5	3.8	INM CM3	3.9
CSIROmk360	4.2	CCCMA CGCM3 T63	3.1
GFDLesm2m	4.3	GFDL CM2.0	6.7

DOI: 10.1038/NGEO1987

GISSe2h	4.6	IPSL CM4	2.1
GISSe2r	4.8	CCCMA CGCM3 T45	3.9
HadCM3	3.6	MPI ECHAM5	2.7
HadGEM2cc	3.7	MIUB ECHO	4.2
HadGEM2es	3.5	CNRM CM3	6.5
Inmcm4	1.0	IAP FGOALS1	2.0
IPSLcm5alr	0.2	UKMO HadGEM1	4.1
MIROC4h	0.2	UKMO HadCM3	3.7
MIROC5	2.9	NCAR CCSM3	5.6
MIROCchem	5.7		
MIROCesm	5.7		
MPIesmlr	2.4		
MRIcgcm3	6.3		

Table S1. The hemispheric asymmetry of upward surface flux in models from Coupled Model Intercomparison Project Phase 5 and Phase 3 (CMIP5 and CMIP3). Fluxes from CMIP5 are calculated by 20 years average from year 1985 to year 2004 in historical simulations. Fluxes from CMIP3 are calculated by 20 years average from year 1980 to year 1999 in 20th century climate simulations.

Supplementary References

S1. Levitus, S., et al. World ocean heat content and thermosteric sea level change (0–2000 m) 1955–2010. *Geophys. Res. Lett.* **39**, L10603 (2012).

S2. Lumpkin, R. & Speer, K. Global ocean meridional overturning. *J. Phys. Oceanogr.* **37**, 2550–2562 (2007).

S3. Ganachaud, A. & Wunsch, C. Large scale ocean heat and freshwater transports during the World Ocean Circulation Experiment. *J. Clim.* **16**, 696-705 (2003).

S4. Talley, L. D. Shallow, intermediate and deep overturning components of the global heat budget. *J. Phys. Oceanogr.* **33**, 530-560 (2003).

S5. Anderson, J. L. et al. The new GFDL global atmosphere and land model AM2–LM2: Evaluation with prescribed SST simulations. *J. Clim*. **17**, 4641–4673 (2004).

S6. Kang, S. M., Held, I. M., Frierson, D. M. W, & Zhao, M. The response of the ITCZ to extratropical thermal forcing: idealized slab-ocean experiments with a GCM. *J. Clim.* **21**, 3521–3532 (2008).

S7. Kang, S. M., Frierson, D. M. W., & Held, I. M. The tropical response to extratropical thermal forcing in an idealized GCM: The importance of radiative feedbacks and convective parameterization. *J. Atmos. Sci*. **66** 2812–2827 (2009).

S8. Kang, S. M., Held, I. M., & Xie, S.-P. Tropical responses to zonally asymmetric thermal forcing, *Climate Dynamics*, in press.

S9. Trenberth, K. E. & Caron, J.M. Estimates of meridional atmosphere and ocean heat transports. *J. Clim.* **14** 3433-3443 (2001)

S10. Fasullo, J. T. & K. E. Trenberth, K.E. The annual cycle of the energy budget: Meridional structures and poleward transports, *J. Clim*. **21**, 10, 2314-2326 (2008).